Available online at www.CivileJournal.org

Civil Engineering Journal

Vol. 5, No. 7, July, 2019

Fatigue Analysis for Void Repair of Cement Concrete Pavement with Under Slab by Polymer Grouting

Can Cui [a], Chengchao Guo [a, b*], Fuming Wang [a]

[a] *School of Water Conservancy and Environment, Zhengzhou University, Zhengzhou 450001, China.*

[b] *School of Civil Engineering, Sun Yat-sen University, Guangzhou 510275, China.*

Received 02 May 2019; Accepted 05 July 2019

Abstract

After the appearing of voids beneath cement concrete slabs, the pavement loses a continuous and uniform lower support structure, and the stress state of the road panel is extremely unfavorable. The polymer grouting repair is timesaving, efficient and pollution-free. In order to verify the performance improvement and fatigue damage evolution of cement concrete pavement before and after grouting repair, a material damage constitutive model was established. The UMAT subprogram was introduced into the finite element software ABAQUS to analyze the structure under the action of moving cyclic loading, stress response and fatigue damage evolution process before and after regional grouting repair. The results show that the Mises stress and vertical displacement of the grouting repairing slab are very close to the normal state, which indicates that the grouting repair has a prominent influence on the bottom void of the slab. With the rise of loading time, the fatigue damage of the pavement structure is increasing, but the trend is gradually reduced, and the number of load times and the degree of fatigue damage are nonlinear. From the long-term cyclic loading and comprehensive analysis of the construction period, the polymer grouting repair is better than cementitious grout.

Keywords: Cement Concrete Pavement; Void under Slab; Polymer Grouting; Fatigue Constitutive Model; Fatigue Damage.

1. Introduction

Cement concrete pavement has many good features and is a high-grade pavement with excellent performance. However, in operation, due to the repeated action of the vehicle loads, the underlying foundation will have a certain plastic deformation. Or the concrete slab will be warped due to the influence of temperature, so that the local extent of the concrete slab is no longer in continuous contact with the foundation. That is, there is a partial void under the concrete slab. The force on the concrete slab is extremely unfavourable. Under the action of the load, the edge of the vacant part will produce local stress concentration, and the repeated load of the heavy traffic will eventually lead to the rupture of the slab, thus affect the functioning condition of the road surface [1].

Polyurethane is one of the largest polymer products in the plastics range. In the past few decades, the use of polyurethane materials to repair and strengthen civil engineering infrastructure has become very widespread [2]. Because it has adhesive properties with other materials, as well as self-supporting features that do not require additional adhesives. This material has been widely used in highways, urban roads, maintenance of airport runways, foundation reinforcement, dam seepage prevention, high-speed rail uplift and other engineering fields [3-4].

Kai Liu et al. (2019) [5] researched that the rigid polyurethane grout materials with different densities show elastoplastic or atypical brittle characteristic, which will significantly affect their performance. Although the

* Corresponding author: chengchao_guo@163.com

http://dx.doi.org/10.28991/cej-2019-03091344

polyurethane material [6] has a significant repair effect on the voids beneath the cement concrete slabs, there is still no theoretical research on the timeliness of the overall performance recovery of the pavement after repairing, fatigue damage analysis and life recovery prediction. In this paper, for the cement concrete pavement with void under slab, the stress and strain mechanical response analysis of the slab before and after grouting is firstly carried out, and then the fatigue constitutive model of four materials: concrete, polyurethane foam [7-8], cementitious, steel, is respectively established [9], introduced into ABAQUS finite element simulation software by UMAT subroutine programming [10], calculate the size of the damage factor [9], analyze the performance improvement and life extension of the pavement before and after grouting repair. Research methodology shows in Figure1.

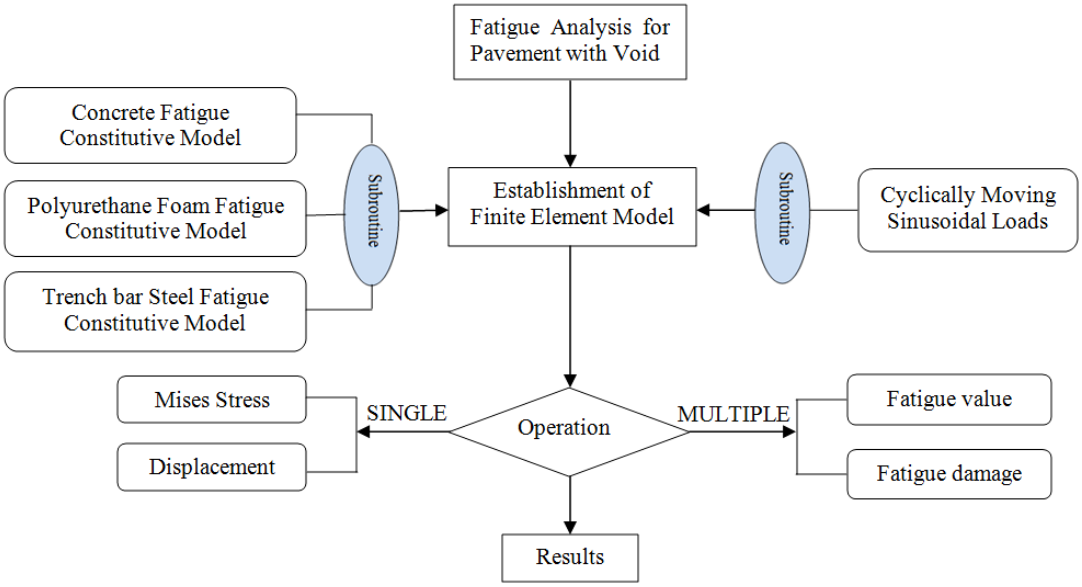

Figure 1. Flowchart of research methodology

Arooran S. et al. (2018) [11] developed measures to minimiza the early-age fatigue damage of prematurely-opened cement-treated due to repective heavy traffic loading. Jianming Ling, et al. (2019) [12] accelerated pavement testing and a finite element method were employed to investigate the effects of three influential factors: temperature, interface bonding, and load level. In the process of cement concrete pavement maintenance, a fatigue model suitable for cement concrete and polymer is proposed, and the failure test of the cyclically moving on the road slab is involved. Especially, the stable relationship between road maintenance and the growth of road service life is obtained, which has a good physical and theoretical foundation for practical engineering.

2. Accumulated Model of Fatigue Damage Evolution

2.1. Concrete Fatigue Constitutive Model

Based on the contact medium damage mechanics and the thermodynamic dissipation theory, Chaboche [13] proposed fatigue constitutive model. This nonlinear fatigue damage evolution model, Equation 1 is used in this paper and used in finite element calculation.

$$\frac{dD}{dN} = A\left(\frac{\sigma}{1-D}\right)^{p}(1-D)^{-q} \tag{1}$$

Where, A, p, q are experimental parameters, usually the material, q can take 0, then the model is simplified to:

$$\frac{dD}{dN} = A\left(\frac{\sigma}{1-D}\right)^{p} \tag{2}$$

It indicates that the damage caused to the material during the Nth cyclic loading is mainly determined by the load stress σ of the Nth cyclic loading and the current damage D. The boundary condition of the model is that D = 0 when n= 0; D = 1 when n = N. Therefore, for the Equation 2 integral, there is:

$$N = \frac{1}{A}\left(\frac{1}{\sigma}\right)^{p}\int_0^1(1-D)^{p}dD = \frac{1}{A(p+1)}\left(\frac{1}{\sigma}\right)^{p} \tag{3}$$

$$n = \frac{1}{A}\left(\frac{1}{\sigma}\right)^{p}\int_0^D(1-D)^{p}dD = \frac{1}{A(p+1)}\left(\frac{1}{\sigma}\right)^{p}\left(1-(1-D)^{p+1}\right) \tag{4}$$

The Equation 3 is divided by the Equation 4:

$$D = 1 - \left(1 - \frac{n}{N}\right)^{\frac{1}{1+p}} \tag{5}$$

On the basis of the formula, Professor Zhao Yongli of Southeast University derived the fatigue constitutive model of concrete with the change of the actual stress ratio, and obtained the modified fatigue constitutive model of concrete:

$$D = 1 - \frac{1}{1 - \frac{(1-\rho)\beta}{R}\lg\left(1 - \frac{n}{N}\right)} \tag{6}$$

β is the experimental parameter, Professor Zhao recommended β taking 0.0640, N is the fatigue life of concrete.

2.2. Polyurethane Foam Fatigue Constitutive Model

The characteristic is observed to show three-stage fatigue characteristic of polymer materials during compression, Wei Y. et al., (2017) [14] that is, the first stage from the beginning of loading to about 100 times, fatigue damage D and elastic strain $\bar{\varepsilon}^{n}$ are directly related, and deformation occurs at the microscopic scale; in the second stage, after about 100 load cycles, the elastic strain is stable and the fatigue damage D is relatively stable; in the third stage, the response of the material under load is drastically changed, about after 1000-2500 load cycles, the plastic phase is entered, the strain value is greater than 5%, which is into damaging step.

Ditho Pulungan and Netherlands (2018) [7], proposed a viscoelastic-viscoplastic model of a polymer that is suitable for various thermoplastic polymers. The constitutive equation was verified by a three-point bending test.

According to the classical continuous damage mechanics, the effective stress tensor and strain tensor are:

$$\tilde{\sigma} = \frac{\sigma}{1-D}, \ \tilde{\varepsilon} = \varepsilon \tag{7}$$

Considering the relationship between stress and relative plastic displacement, there are:

$$\mathrm{D} = \mathrm{D}(\bar{\mu}^{\mathrm{vp}}) \tag{8}$$

Among them;

$$\bar{\mu}^{\mathrm{vp}} = \mathrm{L_c}\left(\bar{\varepsilon}^{\mathrm{vp}} - \bar{\varepsilon}^{\mathrm{vp}}_{\mathrm{D=0}}\right) \tag{9}$$

Therefore, in order to calculate the damage factor D in Equation 8, it is necessary to determine the evolution of the effective plastic displacement $\bar{\mu}^{\mathrm{vp}}$ in Equation 9. Due to the characteristics of the material's brittleness themselves, it is assumed that the two evolve linearly. Therefore, the damage evolution is completely determined by $\bar{\mu}^{\mathrm{vp}}$.

2.3. Trench Bar Steel Fatigue Constitutive Model

Generally, the stress level of high-cycle fatigue of steel bars is low, the yield strength cannot reach, thus the stress and deformation are basically in the elastic phase. Therefore, it is commonly considered that the elastic modulus of steel bars does not degrade during the whole fatigue loading process. According to Miner's linear cumulative damage criterion, the effective cross-sectional area of the steel bar after obtaining N times of fatigue can be calculated by the following Equation 10,

$$\mathrm{A_s^f} = \mathrm{A_s}\left[1 - \frac{\mathrm{N}}{\mathrm{N_f}}\left(1 - \frac{\sigma_{\mathrm{s,max}}}{\mathrm{f_y}}\right)\right] \tag{10}$$

Where $\mathrm{A_s}$ is the initial cross-sectional area of the steel bar, $\mathrm{f_y}$ is the yield strength of the ordinary steel bar, and $\sigma_{\mathrm{s,max}}$ is the maximum stress value of the steel bar during fatigue loading.

$$\mathrm{f_{s,N}} \times \mathrm{A_s} = \mathrm{f_y A_s^f} \tag{11}$$

Substituting Equation 10 into 11, the effective area can be converted into the residual fatigue strength $\mathrm{f_{s,N}}$ of the steel bar. Based on the ideal elastic model of steel bars, the equivalent residual yield strength$\mathrm{f_{y,N}}$ is considered to be equal to the equivalent residual fatigue strength $\mathrm{f_{s,max}}$, shows in Equation 12,

$$f_{s,N} = f_y\left[1 - \frac{N}{N_f}\left(1 - \frac{\sigma_{s,max}}{f_y}\right)\right] \quad (12)$$

3. Establishment of Finite Element Model

3.1. Description of the Model

The model size is length × width × height = 25.4×12.2×10.56 m, slab size is 5×4.2 m, horizontal and longitudinal force transmission rods are arranged between the slabs, each pole is 0.41 m long and 0.3 m apart. The road structure is divided into surface layer, base layer, subbase layer and soil foundation. The surface layer adopts Chaboche fatigue damage constitutive structure, the base layer and the subbase layer adopt linear elastic constitutive, and the soil base adopts Mohr-Coulomb constitutive structure (material parameters are as shown in Table 1.), set 2 cm in length and 0.2 cm in depth at the corner of the center slab to simulate the slab with void underneath (Figure 2a is the overall structural model, Figure 2b is the overall structural mesh).

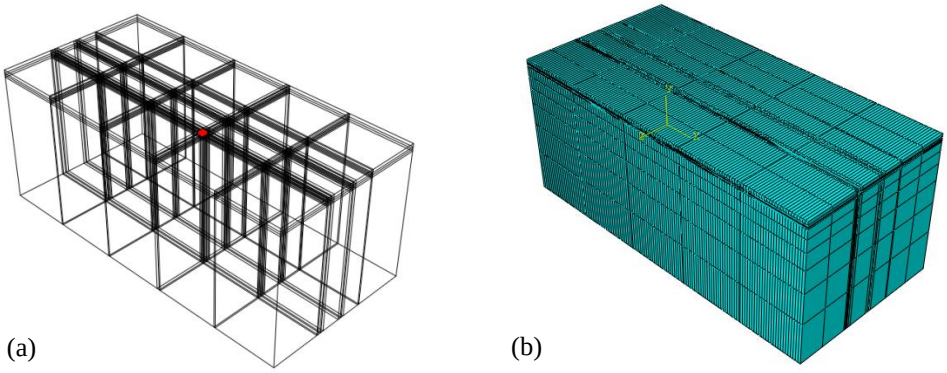

(a) (b)

Figure 2. a) Overall structure calculation model; b) Integral structure mesh

Table 1. Material Parameters

Material	P/Kg·m^{-3}	E/MPa	u_v	C/KPa	φ/°	Δφ/°
24cm cement concrete	2390	3250	0.20	—	—	—
16cm cement stabilized gravel	2300	500	0.25	—	—	—
16cm cement stabilized gravel	1800	200	0.30	—	—	—
Reinforcement	7500	20000	0.30	—	—	—
Asphalt concrete joint material	—	1000	0.25	—	—	—
Soil base	1920	50	0.35	40	22	0
High polymer (Mingsheng Shi (2011))	200	50	0.30	—	—	—

3.2. Contact and Boundary Conditions

The displacement and rotation at the bottom of the model in XYZ directions is restricted. The displacement in the X direction and the rotation in the YZ direction are restricted at the left and right sides, and the displacement in the Y direction and the rotation in the XZ direction are restricted in the front and rear sides. Various structural layers are generally between full sliding and completely continuation in the actual road surface.

3.3. Cyclically Moving Sinusoidal Loads

Standard axle load for high-grade cement concrete pavement is 0.7 MPa in China, which is a double-circle vertical even load. However, during the service of the road, the load is often exceeded the standard value, so in addition to calculating the mechanical response of the standard axle load, the fatigue damage under the overload condition (1.2 MPa -1.8 MPa) should also be calculated. In order to simulate the movement of the load during the calculation, the load moving belt is first set along the moving direction of the load. The width of the moving belt along the lateral direction is the same as the width of the applied sinusoidal load. The length of the moving belt along the longitudinal direction is the distance travelled by the wheel. In order to simulate the most unfavourable state, the load is directly above the void area.

4. User Material Subroutine Development and Application

On the user subroutine interface provided by ABAQUS, the user subroutine UMAT is compiled by FORTRAN95, and the constitutive model of the coupled fatigue damage factor is developed twice.

In this paper, the full-coupling method is mainly used for fatigue damage analysis, that is, the damage field of the structure is updated after each loading, so as to ensure the stress and strain redistribution during the next loading. The calculation flow is shown in the Figure 3.

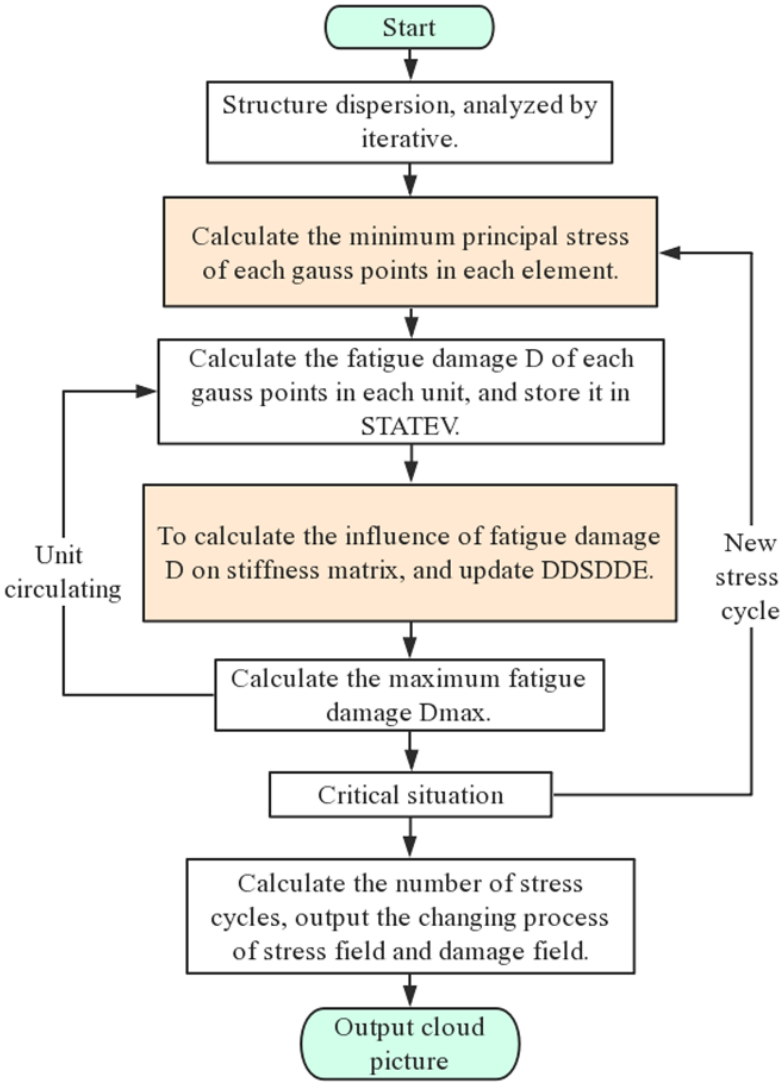

Figure 3. Fully coupled fatigue damage analysis flow chart

According to Equations 2 and 5 and flow in Figure 3, the code of USDFLD based on the finite element calculation for the concrete fatigue constitutive model is built.

5. Result Analysis

5.1. Analysis of Mechanical Response of Different Paths under Moving Loads

In order to study the stress response of the void area, 0.7 MPa was set as standard axle load above the void area moving back and forth, the four working condition: normal, slab with void, repaired void areas with inject polymer foam and cementitious grout, were contrastively analyzed, thus came the Mises stress diagram shown below in Figures 4 and 5, and vertical displacement of concrete slabs show in Figures 6 and 7. Path 2 is the edge of the slab where the load passes through, and path 1 is the inner path of the uniaxial double-wheel group tire.

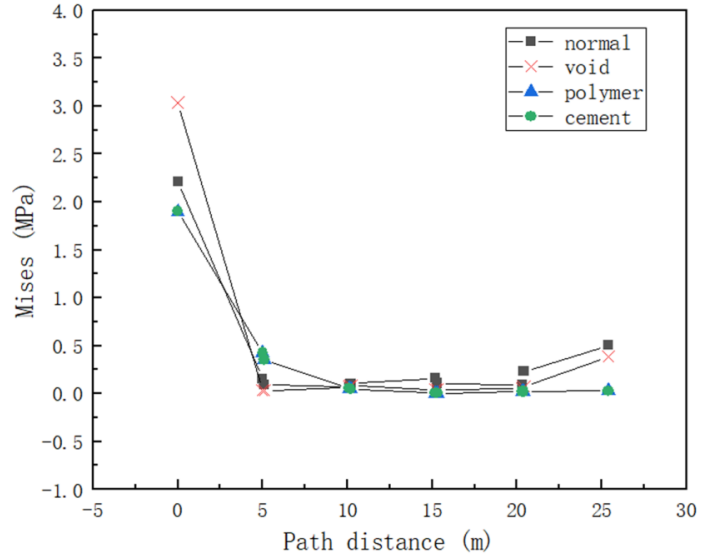

Figure 4. Mises stress curve (Path1)

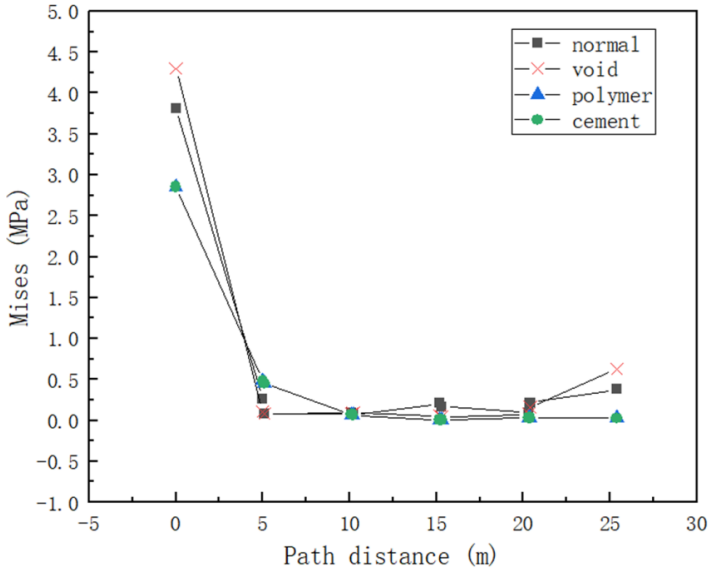

Figure 5. Mises stress curve (Path2)

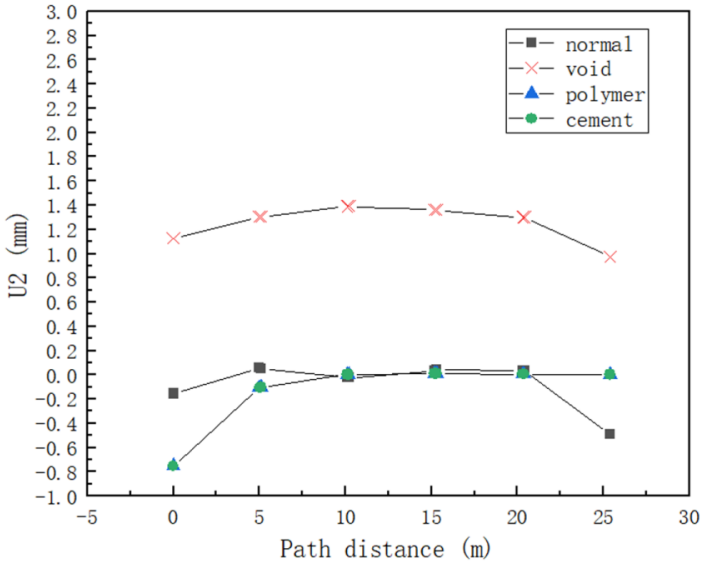

Figure 6. Comparison curve of vertical displacement of concrete slabs (Path1)

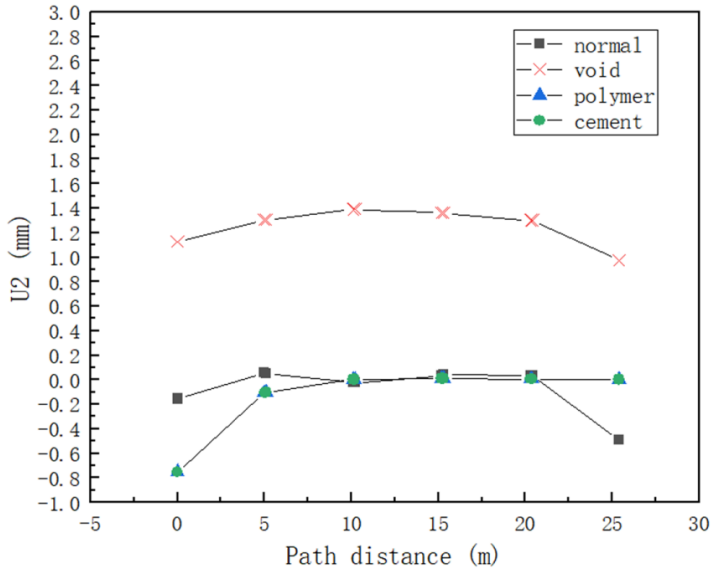

Figure 7. Comparison curve of vertical displacement of concrete slabs (Path2)

It can be seen from Figures 4 and 5 that under the standard axle load, since the initial loading speed is too fast, stress concentration is very likely to occur. After driving the first slab, the stress value is relatively stable. Approaching the edge of the last slab, the stress value rises slightly. It can be seen from the figure that the Mises stress at the edge of the concrete slab is greater than the stress inside the slab, which explains why it is easier to have various diseases at the edge of the slab. In addition, the Mises stress at the bottom of the slab is significantly higher than the other three states in the initial stage and the later stage of loading. In the middle of normal driving area, the Mises stress values of the four states tend to be stable.

It can be seen from Figures 6 and 7 that the vertical displacement value of the bottom void is obviously higher than the other three cases, and the maximum value reaches 1.4 mm, which is very likely to cause cracks and damage of the concrete slab. In addition, it can be seen from Figures 2a and 3 that the Mises stress and vertical displacement of the polymer and cement concrete repairing slabs are very close to the normal state of the concrete panel, indicating that both the polymer material and the cement concrete material has a good repair effect to the bottom void of the slab.

5.2. Time-dependent Response Analysis of Mises Stress in the Position of the Void

In order to analyze the trend of the Mises stress in the void area with time, the Mises stress map is drawn by selecting the same position at the bottom of the four states of the slabs with void, as shown in Figure 5.

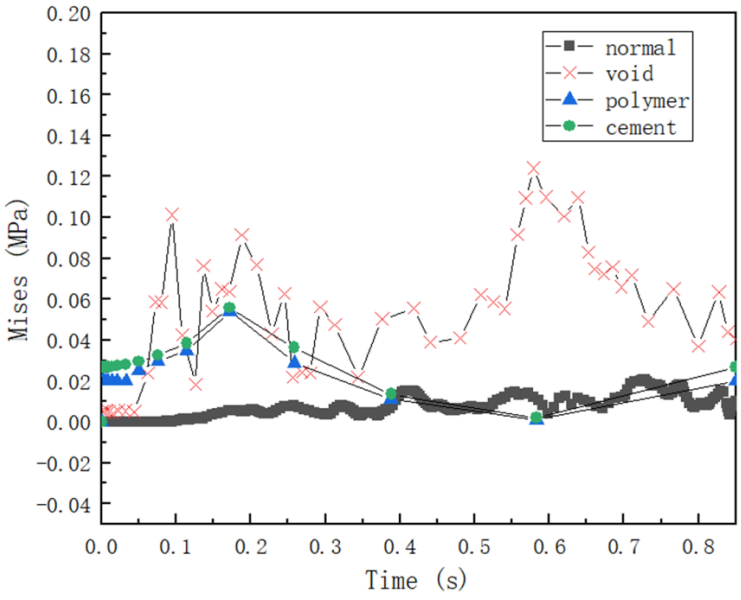

Figure 8. Mises stress contrast curve in the void position

It can be seen from Figure 8 that the maximum Mises stress of the bottom void is 0.13 MPa, which is about 0.12 MPa higher than the normal stress value, indicating that the void has a great influence on the mechanical response of

the concrete slab. At the same time, it can be seen that the Mises stress value decreases by 50-80% before and after the grouting repairing of the void position, and the Mises stress value begins to decrease at 0.4 s, that is, when the load is running directly above the position with void, and then even less than the normal state, grouting repair can effectively reduce the stress value of the bottom of the slab.

5.3. Time History Analysis of Overall Road Dynamic Response

In order to study the development law of the overall mechanical response of cement concrete road with time, we analyze the Mises stress and the maximum curve of vertical displacement of the model. The time history curve is shown in Figures 9 and 10.

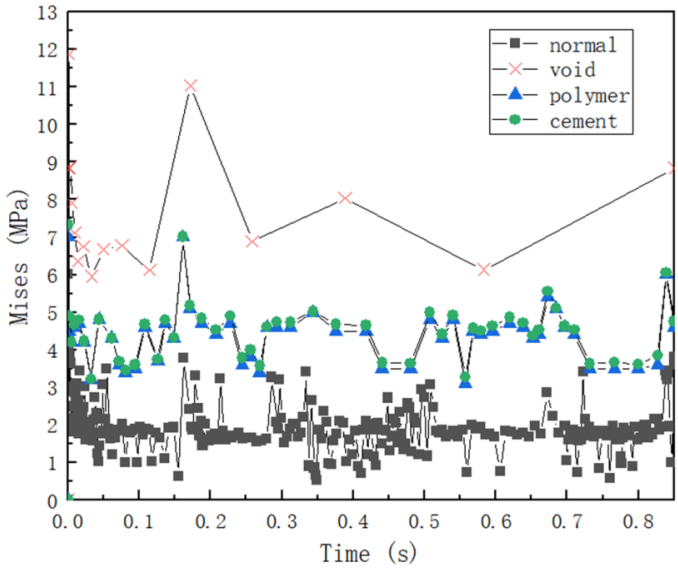

Figure 9. Mises stress time history curve

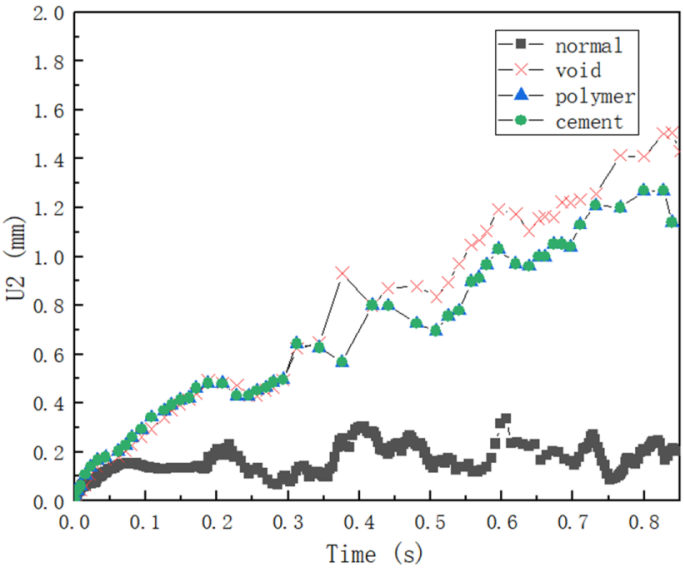

Figure 10. Vertical displacement time history curve

Because the applied load is a wave load, the Mises stress also shows a waveform development trend. Unlike Figure 6, the vertical displacement gradually increases during the load time, because the concrete panel is still elastic during the load time. At the stage, while Figure 10 comprehensively considers various structures such as the force-transmitting rod, the cement stabilized base layer, and the soil foundation, the vertical displacement has a steady upward trend, but the vertical displacement trend under multiple loads needs to be increased duration.

5.4. Fatigue Damage Analysis

Under the action of 1.4 MPa load cycle, the fatigue damage of cement concrete pavement is generated. With the repetition of the load, the damage will continue to develop until the occurrence of macroscopic cracks. Assuming that

the fatigue damage degree at the time of crack formation is 0.5 [9], the red area indicates that macro cracks first appears here. As the model of the reference pavement result of the void area is enlarged, it can be seen that when the repeated loads acted 560,000 times, 980,000 times, 1.2 million times, 1.68 million times, 2.15 million times, 2.98 million times, 3.28 million times, 4.06 million times and 4.36 million times respectively, the post-injury factor increases from 0.0003 to 0.52.

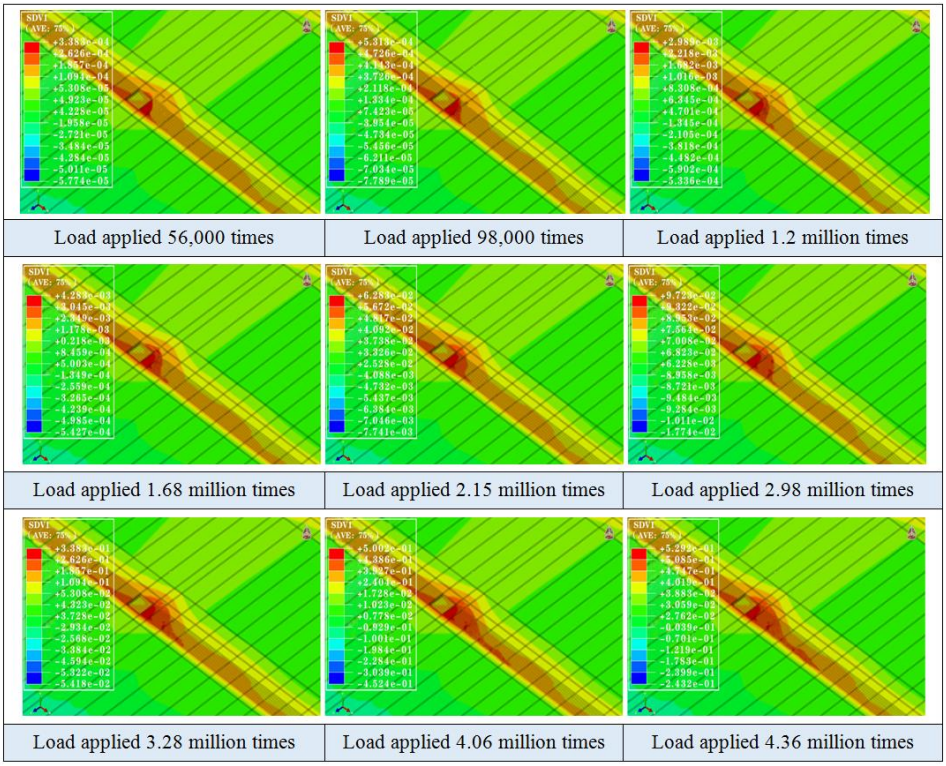

Figure 11. Variation of Fatigue Damage Field Distribution in Reference Pavement Structure Model

In order to quantitatively analyze the distribution law of the fatigue damage field of the reference pavement structure, the reference pavement structure with the repeated load acting 4.36 million times is taken as the object, the unit integration point with the damage factor reaching 0.46 is taken as the origin, and the three-dimensional coordinate system is established, with vehicle travel direction in the X direction, the vertical vehicle travel direction in the Y direction, and the gravity direction in the Z direction. At this time, the distribution of the fatigue damage field in the reference pavement structure model on the X-axis, Y-axis, and Z-axis is as shown in Figure 12 to 14.

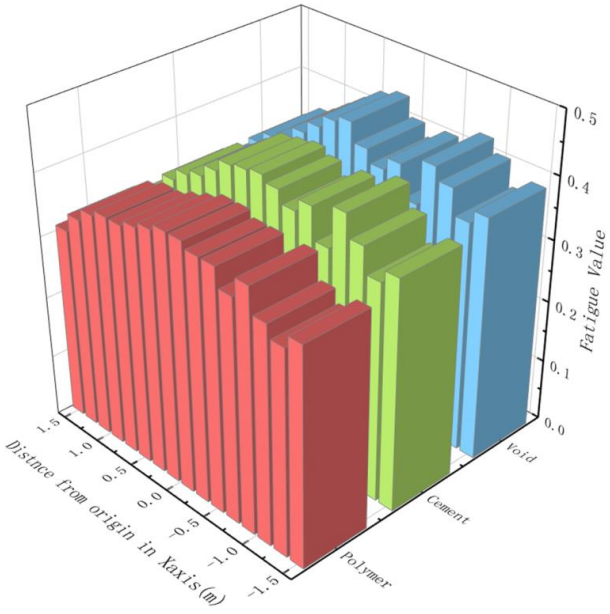

Figure 12. Damage distribution of the top surface in the X-axis

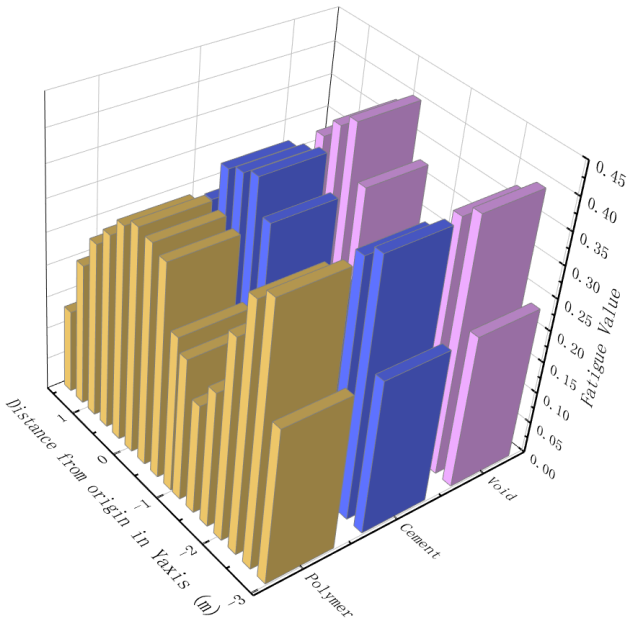

Figure 13. Damage distribution of the top surface in the Y-axis

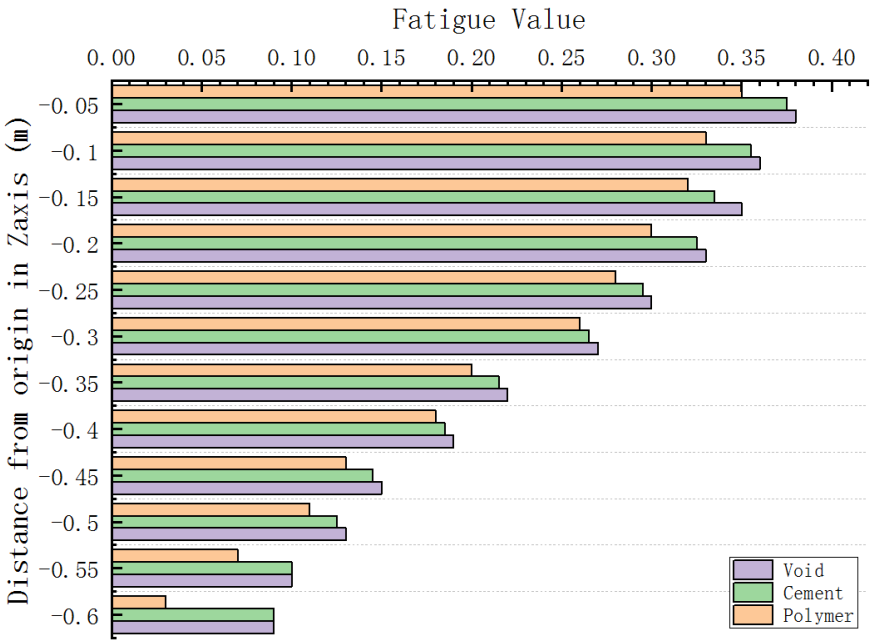

Figure 14. Damage distribution of the top surface in the Z-axis

It can be seen from Figure 9 that after loading millions of times along the road travel direction, the fatigue damage factor value of the three models is high, the regional damage threshold is 0.5, and the value of the surface layer directly above the void area peaks. After the polymer grouting repair and cement slurry repair, the value of the fatigue damage factor directly above the void area is significantly reduced, and the former is smaller than the latter. It can be seen from Figure 10 that in the direction of vertical vehicle travel, the fatigue damage factor appears in the form of a double peak curve, that is, the road damage is more serious at the wheel track. It can be seen from Figure 11 that the fatigue damage factor value is extended downward and gradually decreases, and the influence range is from the surface layer to 0.6 m below the surface layer, that is, the repeated motion mechanics of the vehicle load is in the structural layer above the base layer. It can be clearly seen that the fatigue damage factor value of polymer grouting repair is significantly lower than the other two working conditions, which indicates that the long-term performance of polymer grouting repair is higher than that of cement slurry under the load of 1.4 MPa tire pressure repair. However, related research shows that polymer grouting repair can only strengthen the base layer and prolong the service life of the road, but the smoothness of the surface layer and the comfort of driving cannot be improved.

Under cyclic loading, fatigue damage of cement concrete road appears, and as the load continues to develop, this

damage continues to develop until macroscopic cracks appear. Taking the reference pavement structure model under the repeated load as an example, the fatigue damage degree changes with the load acting times as shown in Figure 15 to 18.

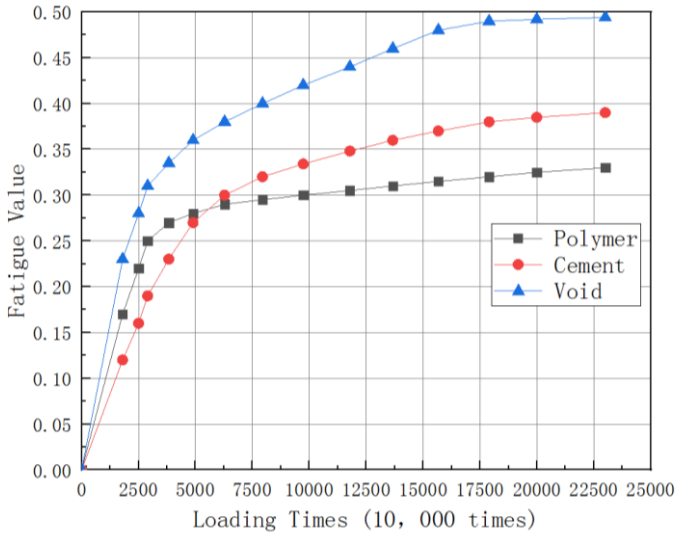

Figure 15. Tire grounding pressure 1.2 MPa

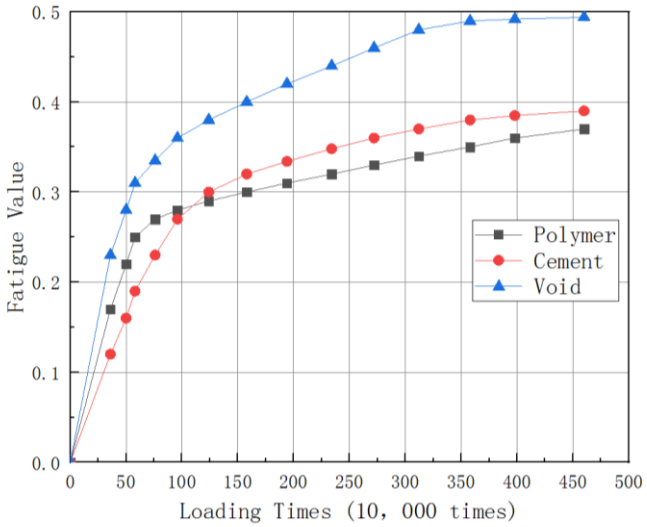

Figure 16. Tire grounding pressure 1.4 MPa

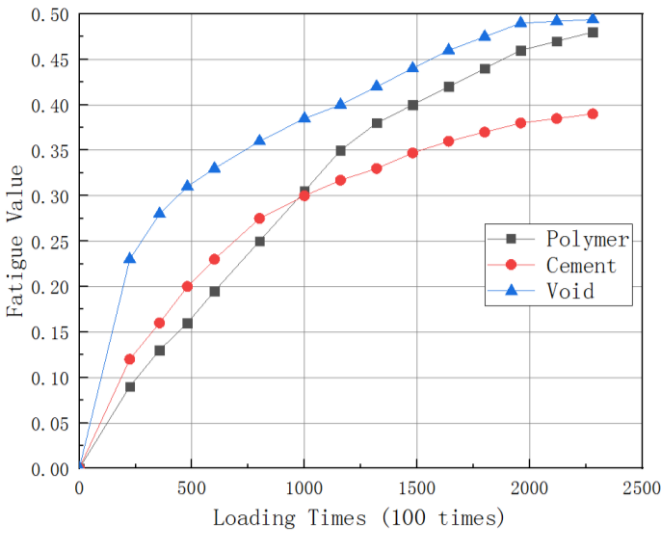

Figure 17. Tire grounding pressure 1.6 MPa

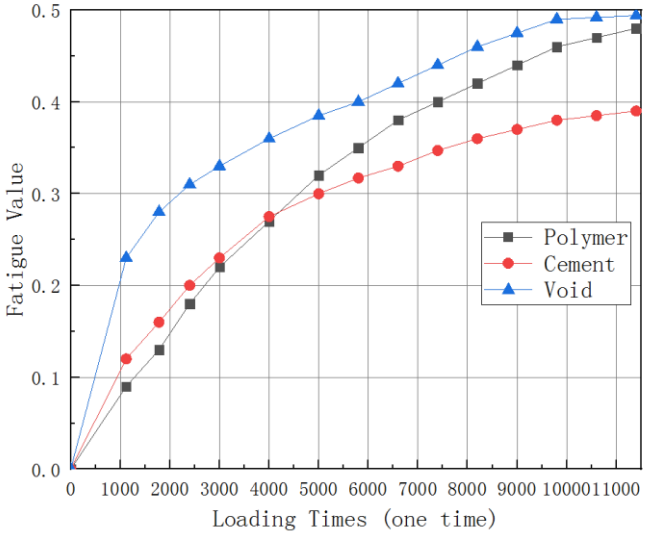

Figure 18. Tire grounding pressure 1.8 MPa

In the finite element calculation, the interaction between the load stress field and the fatigue damage field is considered. The coupling of the two fields will lead to the continuous change of the load stress field. Therefore, the fatigue damage degree at the origin of the top surface of the panel presents a nonlinear feature with the increasing number of load times.

It can be seen from Figures 15 to 18 that the fatigue damage degree at the origin of the top surface of the panel rises with the increasing times of load. At the same time, the greater the grounding pressure of the tire, the less corresponding load times fatigue damage degree of the pavement structure reaches 0.5. Taking reference pavement structure model with void under repeated action of 1.2 MPa of the tire grounding pressure in the Figure 16 as the example, when the load is applied 610,000 times, the fatigue damage degree develops to 0.3, and when the load increases from 610,000 times to 1.59 million times, the fatigue The damage degree has been newly developed by 0.1, to 0.4, when the load has reached 4.6 million times from 1.59 million times, the fatigue damage degree finally develops to 0.5. Obviously, as the number of times of load increases, the amplification of fatigue damage degree at the origin of the panel top surface of decreases.

It can be seen from Figure 15 and 16 that in the pavement structure model with void the fatigue damage degree develops rapidly. At the initial stage of load, slow development of fatigue damage factor of the pavement structure model after cement slurry repair and polymer grouting can be seen. After the grounding pressure of 1.2 MPa 50.02 million times and the tire grounding pressure of 1.2 MPa 1.17 million times, the pavement structure model of polymer grouting repair shows the advantage that the damage factor value is smaller than the road structure model of cement slurry repair, which is because it is in the elastic phase of the second stage at this time (the three-stage fatigue of the polymer [15] labor damage process), that is, the microscopic pores are gradually reduced, but the stage of damage has not yet occurred. It can be seen from Figures 14 and 15 that as the of the tire grounding pressure increases, the fatigue damage of the polymer material develops from the second stage to the third, after tire grounding pressure of 1.6 MPa 100,000 times and tire grounding pressure 1.8 MPa 4010 times. In this stage, the failure stage, micro-cracks begin to appear because the polymer material itself has a low bearing capacity and is prone to deformation under large loads.

Therefore, through the finite element calculation of the road structure model, it can be known the fatigue damage develops rapidly when the void under slab of the cement concrete road is generated, and needs to be repaired in time to prevent large-area cracks in the panel. Under the action of general road load (<1.6 MPa), the polymer grouting repair method can effectively reduce the fatigue damage degree, but in the heavy-duty road area, it needs to be repaired with cement slurry material. However, considering the traffic-close hour of maintenance, that the polymer repair method is less than 4 hours, and the cement slurry repair method is more than 3 days, in terms of the repair method of void under high-grade cement concrete road and the base layer loose, the polymer grouting repair method is preferred; but in the repair process, it should be combined with the FWD and GPR detection methods, to reasonably determine the amount of grouting, avoiding excessive material injection and causing slab damage.

6. Conclusions

- For the repair of void under slab of cement concrete roads, both high polymer materials and cement concrete materials are of good effect, and can effectively reduce the stress value of the slab bottom.
- Under the 0.7 MPa standard axle load, the Muses stress value of the void position under polymer grouting before and after the repair is reduced by 50%-80%.

- Under the multiple loads, the road damage at the load track is more serious, and the longitudinal influence area starts from the surface layer to 0.6 meters below the surface layer.
- Under the action of general road load (<1.6 MPa), the polymer grouting repair method can effectively reduce the fatigue damage degree, but in the heavy-duty road area, joint effort from cement slurry material is needed.

7. Funding

Chinese National Key R & D Projects (2016YFC0802200).

8. Conflicts of Interest

The authors declare no conflict of interest.

9. References

[1] Hu, Chunhua, and Shuangshuang Shi. "Summary of the Grouting Material for the Void Beneath Cement Concrete Pavement Slab." IOP Conference Series: Materials Science and Engineering 382 (July 2018): 022096. doi:10.1088/1757-899x/382/2/022096.

[2] Somarathna, H.M.C.C., S.N. Raman, D. Mohotti, A.A. Mutalib, and K.H. Badri. "The Use of Polyurethane for Structural and Infrastructural Engineering Applications: A State-of-the-Art Review." Construction and Building Materials 190 (November 2018): 995–1014. doi:10.1016/j.conbuildmat.2018.09.166.

[3] Guo, Cheng-chao, Wang, Fu-ming, and Zhong, Yan-hui, "Research on grouting technology of hollow concrete in cement concrete pavement." Highway. 10, 10 (2008): 232-236.

[4] Bian, Xue-cheng, Cheng Yu, Wang, Fu-ming, Jiang, Jian-chun, and Chen, Yun-min, "Experimental study on dynamic performance and long-term durability of high-speed railway subgrade settlement after grouting repair." Chinese Journal of Geotechnical Engineering. 03, 36 (2014):562-568.

[5] Liu, Kai, Wei Liang, Fengmei Ren, Jingge Ren, Fang Wang, and Heng Ding. "The Study on Compressive Mechanical Properties of Rigid Polyurethane Grout Materials with Different Densities." Construction and Building Materials 206 (May 2019): 270–278. doi:10.1016/j.conbuildmat.2019.02.012.

[6] Ling, Jianming, Fulu Wei, Hongduo Zhao, Yu Tian, Bingye Han, and Zhi'ang Chen. "Analysis of Airfield Composite Pavement Responses Using Full-Scale Accelerated Pavement Testing and Finite Element Method." Construction and Building Materials 212 (July 2019): 596–606. doi:10.1016/j.conbuildmat.2019.03.336.

[7] Pulungan, Ditho, Arief Yudhanto, Shiva Goutham, Gilles Lubineau, Recep Yaldiz, and Warden Schijve. "Characterizing and Modeling the Pressure- and Rate-Dependent Elastic-Plastic-Damage Behavior of Polypropylene-Based Polymers." Polymer Testing 68 (July 2018): 433–445. doi:10.1016/j.polymertesting.2018.02.024.

[8] Shojaei, Amir K., and Pieter Volgers. "A Coupled Hyperelastic-Plastic-Continuum Damage Model for Studying Cyclic Behavior of Unfilled Engineering Polymers." International Journal of Fatigue 107 (February 2018): 33–39. doi:10.1016/j.ijfatigue.2017.10.006.

[9] Xue, Yan-qing, Huang, Xiao-ming, Shi, Xiao-wu, and Ma Tao, "Fatigue damage mechanism under traffic load of concrete pavement with void." Journal of Southeast University (Natural Science Edition). 01, 44 (2014): 199-204.

[10] Lee, Chi-Seung, and Jae-Myung Lee. "Failure Analysis of Reinforced Polyurethane Foam-Based LNG Insulation Structure Using Damage-Coupled Finite Element Analysis." Composite Structures 107 (January 2014): 231–245. doi:10.1016/j.compstruct.2013.07.044.

[11] Sounthararajah, Arooran, Ha Hong Bui, Nhu Nguyen, Peerapong Jitsangiam, and Jayantha Kodikara. "Early-Age Fatigue Damage Assessment of Cement-Treated Bases Under Repetitive Heavy Traffic Loading." Journal of Materials in Civil Engineering 30, no. 6 (June 2018): 04018079. doi:10.1061/(asce)mt.1943-5533.0002250.

[12] Ling, Jianming, Fulu Wei, Hongduo Zhao, Yu Tian, Bingye Han, and Zhi'ang Chen. "Analysis of Airfield Composite Pavement Responses Using Full-Scale Accelerated Pavement Testing and Finite Element Method." Construction and Building Materials 212 (July 2019): 596–606. doi:10.1016/j.conbuildmat.2019.03.336.

[13] Patil, A. N., and B. M. Dawari. "Chaboche's Viscoplasticity Model for Strain–Space Plasticity." Procedia engineering 173 (2017): 1093-1100. doi:10.1016/j.proeng.2016.12.066

[14] Xiang, Gao, Wei Ya, and W. A. N. G. Fuming and Zhong, Yan-Hui "Fatigue resistant and microstructure evolution of polyurethane grout materials under uniaxial compression." Acta Materiae Compositae Sinica 34, no. 3 (2017): 550-556.

[15] Wei, Ya, Fuming Wang, Xiang Gao, and Yanhui Zhong. "Microstructure and Fatigue Performance of Polyurethane Grout Materials Under Compression." Journal of Materials in Civil Engineering 29, no. 9 (September 2017): 04017101. doi:10.1061/(asce)mt.1943-5533.0001954.